Concentration dependence of the ionic structure and dynamics in metal-salt solutions

1991 J. Phys.: Condens. Matter 3 2583

(http://iopscience.iop.org/0953-8984/3/15/013)

J. Phys.: Condens. Matter 3 (1991) 2583–2588. Printed in the UK

LETTER TO THE EDITOR

Concentration dependence of the ionic structure and dynamics in metal-salt solutions

J-P Hansen† and F Yoshida‡

† Laboratoire de Physique, Unité de Recherche Associée 1325 du CNRS, Ecole Normale Supérieure de Lyon, 69364 Lyon Cédex 07, France

‡ Research Reactor Institute, Kyoto University, Kumatori-cho, Sennan-gun, Osaka 590-04, Japan

Received 7 February 1991

Abstract. A simple screened Coulomb model is used to investigate the crossover from ionic to metallic behaviour of the pair structure and longitudinal collective modes in metal-salt solutions, with specific application to $K_x(KCl)_{1-x}$.

Solutions of alkali metals in their halides are interesting ionic liquids which allow a detailed study of the variation of electron transport and of ionic structure and dynamics with metal concentration, x [1]. The peculiar dependences on x of the partial ionic structure factors [2], and of the excess molar volume [3] reflect the change of the valence electron states [4] and of their screening efficiency in going from the pure metal to the pure salt. While the structural and dynamic properties of pure liquid alkali metals ($x = 1$) and pure molten alkali halides ($x = 0$) are relatively well understood [5], much less theoretical work has been devoted to their mixtures. A simple model, where electrons are treated as a rigid uniform background, leads to a pair structure [6] in qualitative agreement with experiment [2]. A hydrodynamic analysis of the same model leads to unexpected, but inconclusive predictions for the long-wavelength collective modes that appear to be very sensitive to the polarization of the valence electrons [7].

In this letter we introduce a simple model in which the ions interact via a screened Coulomb potential, and the screening length λ varies with the density of valence electrons, i.e. with x. The model is designed to interpolate smoothly between reasonable interaction potentials for pure metal and pure salt. This allows us to investigate the variation of the pair structure with x, and to analyse, for the first time, the evolution of the longitudinal collective modes with metal concentration for wavenumbers k which are accessible to inelastic neutron scattering experiments.

We consider a metal-salt solution $M_x(MX)_{1-x}$, where M denotes the cation, X the anion and x the metal concentration. Treatment will be limited to a fully symmetric system where anions and cations have opposite charge ($\pm e$) and equal mass m; we have in mind the widely studied metal-salt solution $K_x(KCl)_{1-x}$. If n is the total number density of the ions, the corresponding density of the conduction electrons will be $n_0 =$

0953-8984/91/152583 + 06 $03.50

$[x/(2-x)]n$, and a convenient length scale is the ion sphere radius $a = (3/4\pi n)^{1/3}$. The interactions of the ions are described by the following set of model pair potentials:

$$v_{\alpha\beta}(r) = (1 - \delta_{\alpha\beta})B \exp(-Ar) + (Z_\alpha Z_\beta e^2/r)e^{-r/\lambda} \tag{1}$$

where $1 \leqslant \alpha, \beta \leqslant 2$ are species indices and Z_α ($= \pm 1$) is the valence of ion species α. The first term describes the Born–Mayer short-range repulsion between unlike ions; the parameters A and B are chosen identical to those of the Tosi–Fumi potential for the corresponding pure molten salt [8]. The second term on the right hand side of (1) is the screened Coulomb potential between ions. The concentration dependence of λ is chosen to be the same as that of the temperature- and density-dependent Thomas–Fermi (TF) screening length λ_{TF}. In the pure metal ($x = 1$), the temperature T is much less than the electron Fermi temperature T_F, and λ_{TF} reduces to the zero-temperature screening length, $\lambda_{TF} \sim n_0^{-1/6}$. However, in order to achieve good agreement between the calculated and experimental structure factor of the pure metal (see below), we found that λ_{TF} must be rescaled to a somewhat larger value $\lambda = \zeta\lambda_{TF}$; for liquid K at $T \simeq 10^3$ K, the optimum ζ turns out to be 1.6. This rescaling may be regarded as a compensation for the crudeness of the TF description of electron screening. The same scaling factor, ζ, has been kept for all concentrations, x, so that finally, along an isotherm, $\lambda(x) = \zeta\lambda_{TF}(x)$.

For low metal concentrations ($x \to 0$), the electron Fermi temperature $T_F \ll T$, and the TF screening length of the nearly classical electrons reduces to the Debye screening length $\lambda_D \sim n_0^{-1/2}$. For the pure molten salt ($x = 0$), the ion–ion pair potentials (1) reduce to the familiar Tosi–Fumi form, without the Van der Waals dispersion terms, which should have a very minor influence on the ionic pair structure. The latter is characterized by the partial structure factors:

$$S_{\alpha\beta}(k) = \frac{1}{\sqrt{N_\alpha N_\beta}}\langle \rho_{k\alpha}\rho_{-k\beta}\rangle = \delta_{\alpha\beta} + (x_\alpha x_\beta)^{1/2} n \int [g_{\alpha\beta}(r) - 1]\, e^{ik\cdot r}\, dr \tag{2}$$

where N_α and $\rho_{k\alpha}$ denote the number of ions and the Fourier component of the microscopic density of species α, $x_\alpha = N_\alpha/N$ with $N = N_1 + N_2$, while $g_{\alpha\beta}(r)$ denotes the partial pair distribution function between ions of species α and β. We have calculated $S_{\alpha\beta}$ and $g_{\alpha\beta}$ from numerical solutions of the recently proposed HMSA integral equation, which is thermodynamically self-consistent, and has been shown to be remarkably accurate for a wide variety of liquids, including molten salts [9]. In particular the HMSA closure is much more accurate than the familiar HNC closure used in earlier work on metal-salt solutions [6].

In order to check the consistency of our model, we have applied the above procedure to $K_x(KCl)_{1-x}$ solutions. In figure 1 we show the results obtained for the partial structure factors $S_{11}(k) \equiv S_{22}(k)$ and $S_{12}(k)$ of the pure molten salt KCl at $T = 1050$ K, together with the rigid-ion molecular dynamics (MD) data of Dixon and Gillan [10] who used pair potentials identical to (1), except for the inclusion of Van der Waals dispersion terms. The agreement is seen to be excellent. Our HMSA calculations, as well as the simulations, were carried out at the experimental molar volume $V_m = 50$ cm^3. The calculated pressure turns out to be too high ($P = 10.2$ kbar), which is not unexpected since our model omits the Van der Waals attractions between ions; if these are included, the pressure computed from the HMSA integral equation drops to 3.5 kbar, in good agreement with the MD result under identical conditions [10].

The structure factor calculated for pure liquid K at the same temperature is compared with the neutron scattering data of Jal [11] at $T = 973$ K and a molar volume $V_m = 60$ cm^3 in figure 2. Interestingly, the total calculated pressure, including the electronic

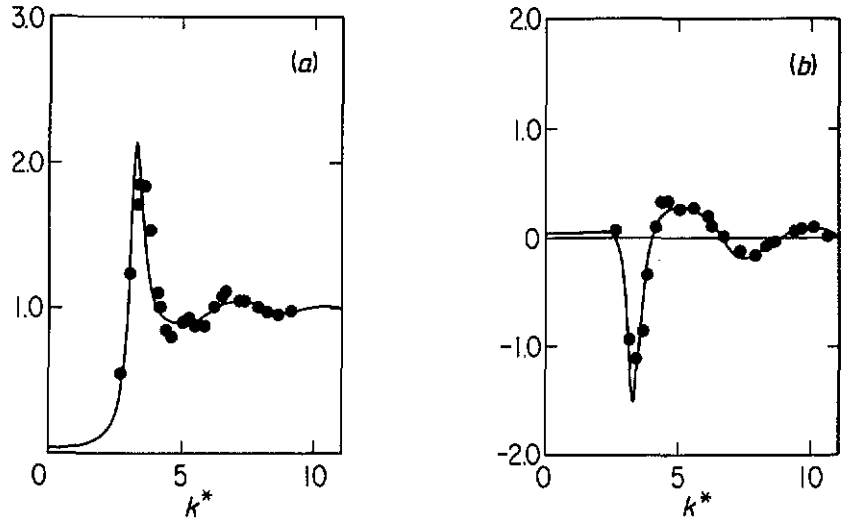

Figure 1. Partial structure factors $(a)\ S_{11}(k)$ and $(b)\ S_{12}(k)$ for the pure salt (KCl), as calculated from the HMSA equation, versus $k^* = ka$, for $T = 1050$ K and $V_m = 50$ cm^3. The full circles are MD data from [10].

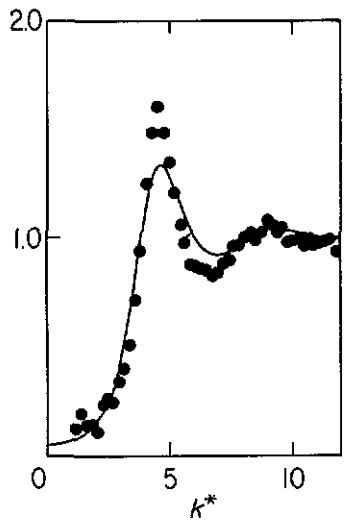

Figure 2. Structure factor $S(k) \equiv S_{11}(k)$ of pure liquid K, as a function of k^* for $T = 1050$ K and $V_m = 60$ cm^3 calculated from the HMSA equation. The full circles are neutron diffraction data [11] for the same volume, and $T = 973$ K.

contribution, is very close to that obtained for pure KCl ($P \simeq 10$ kbar). The results shown in figures 1 and 2 point to the consistency of our model for the two limiting concentrations $x = 0$ and 1. We have extended the HMSA structure calculations to intermediate concentrations x, assuming a linear dependence of the molar volume on x, i.e. ignoring the relatively large excess volumes observed experimentally [3].

The resulting pair structure was used as an input to a generalized Langevin equation analysis of longitudinal collective modes in metal-salt solutions, for wavenumbers k accessible to inelastic neutron scattering experiments [12]. Following the familiar Mori–Zwanzig formalism [5], we chose a dynamical set $\mathbf{A}(k)$ made up of the conserved

variables, namely the local number density, the local charge density, and the longitudinal mass current density, plus the non-conserved longitudinal charge current density:

$$\rho_{kN}(t) = (1/\sqrt{2})[\rho_{k1}(t) + \rho_{k2}(t)] \equiv A_{k1}(t) \tag{3a}$$

$$\rho_{kZ}(t) = (1/\sqrt{2})[\rho_{k1}(t) - \rho_{k2}(t)] \equiv A_{k2}(t) \tag{3b}$$

$$j_{kN}(t) = \dot{\rho}_{kN}/ik \equiv A_{k3}(t) \tag{3c}$$

$$j_{kZ}(t) = \dot{\rho}_{kZ}/ik \equiv A_{k4}(t). \tag{3d}$$

Since the energy density is not included in the basic set of dynamical variables, the present analysis neglects temperature fluctuations, a reasonable approximation for ionic systems.

The 4×4 correlation function matrix has elements $C_{\alpha\beta}(k, t) = \langle A_{k\alpha}(t)A_{-k\beta}(0)\rangle/N$. Its Laplace transform $\tilde{C}(k, z)$ obeys the generalized Langevin equation:

$$[z\delta_{\alpha\gamma} - i\Omega_{\alpha\gamma}(k) + \tilde{M}_{\alpha\gamma}(k, z)]\tilde{C}_{\gamma\beta}(k, z) = C_{\alpha\beta}(k) \tag{4}$$

where summation over repeated indices is implied. The elements $C_{\alpha\beta}(k) = C_{\alpha\beta}(k, t = 0)$ of the static correlation function matrix, and of the secular frequency matrix $\boldsymbol{\Omega}(k)$ are expressible in terms of static quantities. The memory function $\mathbf{M}(k, t)$ is defined as the ratio of the random force autocorrelation function, $R_{\alpha\beta}(k, t) = \langle f_{k\alpha}(t)f_{-k\beta}\rangle/N$, over $C(k)$. With the choice of dynamical variables (3), $f_{k1}(t) = f_{k2}(t) \equiv 0$, and the memory function matrix has only four non-zero elements (M_{33}, M_{34}, M_{43} and M_{44}).

For the random force autocorrelation function matrix $\tilde{\mathbf{R}}(k, z)$ we adopt a simple relaxational *ansatz* based on a low-frequency approximation [13]. Adapting the results of [13] to the present case, we obtain:

$$\tilde{R}_{\alpha\beta}(k, z) = c_{\alpha\beta}(k)/[z + z_3(k)] + d_{\alpha\beta}(k)/[z + z_4(k)] \tag{5}$$

where the coefficients $c_{\alpha\beta}$ and $d_{\alpha\beta}$ are related to the initial values $M_{\alpha\beta}(k) \equiv M_{\alpha\beta}(k, t = 0)$, while z_3 and z_4 are the real positive roots of the determinant, $[z^2\mathbf{I} - \mathbf{M}(k)] = 0$. This entirely determines the memory function matrix $\tilde{\mathbf{M}}$ in (4). Propagating collective modes are signalled by peaks in the spectra $\tilde{C}_{\alpha\beta}(k, \omega) = \lim_{\varepsilon\to 0} R\tilde{C}$ $(z = i\omega + \varepsilon)/\pi$ of the correlation functions; these resonances are associated with the poles of the $\tilde{C}_{\alpha\beta}(k, z)$ satisfying (4) which are the complex roots of the dispersion equation:

$$\begin{aligned} z^4 + [\tilde{M}_{33} + \tilde{M}_{44}]z^3 + [\tilde{M}_{33} - \tilde{M}_{44} - \tilde{M}_{34}\tilde{M}_{43} - (v_0k)^2(S_{11} + S_{22})/\Delta]z^2 \\ + (kv_0^2/\sqrt{2})[\Omega_{31}\tilde{M}_{44} + \Omega_{42}\tilde{M}_{33} - \Omega_{41}\tilde{M}_{34} - \Omega_{32}\tilde{M}_{43}]z \\ + (v_0k)^4/\Delta = 0 \end{aligned} \tag{6}$$

where $\Delta(k) = S_{11}(k)S_{22}(k) - S_{12}^2(k)$ and $v_0^2 = (k_B T/m)$. The elements of the secular frequency matrix $i\boldsymbol{\Omega}$ are all proportional to k and entirely determined by the partial structure factors.

In the pure salt, $(kv_0)^4/\Delta(k)$ approaches $(c_T k)^2\omega_p^2$ in the $k \to 0$ limit, where $c_T = (mn\chi_T)^{-1/2}$ is the isothermal sound velocity (χ_T is the compressibility) and $\omega_p = (4\pi ne^2/m)^{1/2}$ is the plasma frequency. Similarly $(kv_0)^2[S_{11}(k) + S_{22}(k)]/\Delta(k) \simeq \omega_p^2 + O(k^2)$. Hence, neglecting all damping, which amounts to setting $\tilde{\mathbf{M}}(k, z) = 0$ in (6), the dispersion equation admits the solutions $z^2 = (c_T k)^2$ and ω_p^2 to leading order in k, corresponding to long-wavelength sound and optic modes. In the $k \to 0$ limit only the

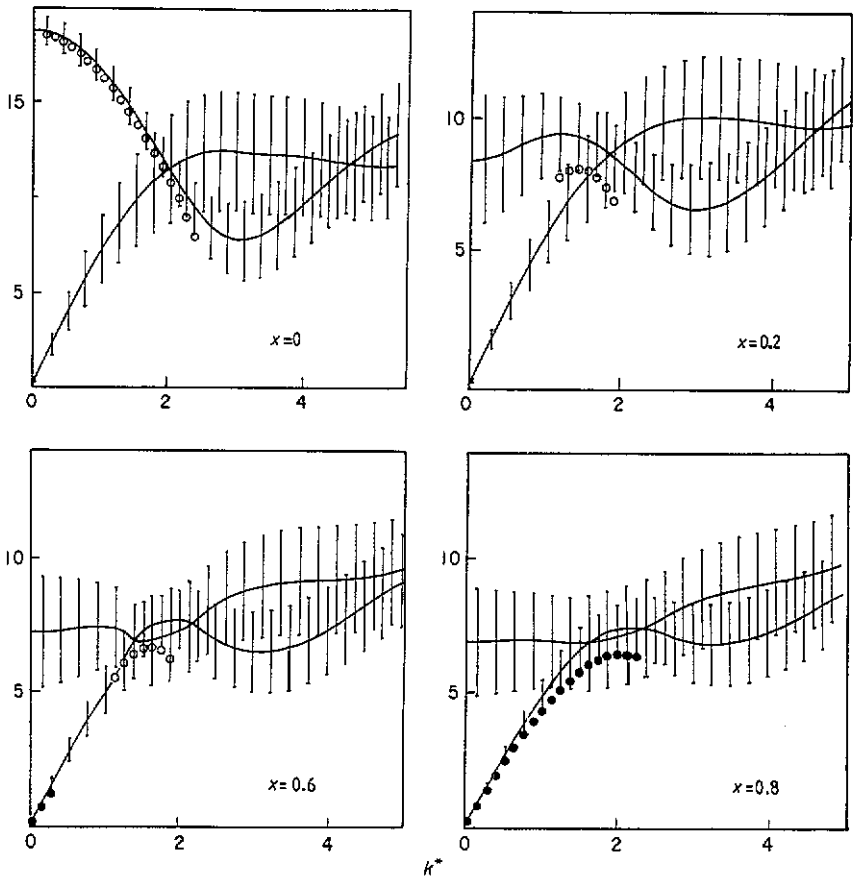

Figure 3. Dispersion curves of the acoustic and optic modes in metal-salt solutions for metal concentrations $x = 0$, 0.2, 0.6 and 0.8. The full curves and vertical bars correspond to the real and imaginary parts of the complex roots of (6) ($z = \omega + i\gamma$). The full and open circles indicate the positions of the peaks in the mass and charge density fluctuation spectra $S_{NN}(k, \omega)$ and $S_{ZZ}(k, \omega)$, respectively.

$\tilde{M}_{44}$ matrix element is non-zero, reflecting the non-conserved nature of the charge current; this leads to an increase of the optic mode frequency above ω_p [5, 8].

In the pure metal, $(kv_0)^2/\Delta(k)$ and $(kv_0)^2[S_{11}(k) + S_{22}(k)]/\Delta(k)$ approach $(kv_0)^2(kc_T)^2$ and $(kv_0)^2 + (c_Tk)^2$, respectively, when $k \to 0$. Neglecting $\tilde{\mathbf{M}}(k, z)$ in (6), the dispersion equation yields the two roots $z^2 = (c_Tk)^2$ and $(v_0k)^2$; the first is the usual sound mode, while the second has no physical significance for $x = 1$. However, for intermediate concentrations ($0 < x < 1$), both $\tilde{M}_{43}(k \to 0, z)$ and $\tilde{M}_{44}(k \to 0, z)$ are non-zero. These have a drastic effect on the pole at $(kv_0)^2$, which is changed into a high-frequency optic mode for all $x < 1$.

For finite values of k, we have used the HMSA output to compute the k-dependent coefficients in (5) and (6). The resulting dispersion curves, with vertical bars representing the imaginary part of the roots, characterizing the damping, are plotted in figure 3, for four concentrations, x. The optic mode frequency drops rapidly below its pure salt value as x increases, and the optic and acoustic branches cross at $k^* = ka \simeq 2$, so that interference effects are to be expected in the intermediate wavenumber range.

The same figure also shows the positions of the peaks observed in the mass (or density) fluctuation spectrum $S_{NN}(k, \omega) \equiv \hat{C}_{11}(k, \omega)$ (for the acoustic mode), and in the charge fluctuation spectrum $S_{ZZ}(k, \omega)$ (for the optic mode), as a function of k. In the pure metal, the sound peak in $S_{NN}(k, \omega)$ is well defined up to $k^* = k_m^* \simeq 2.9$, where it vanishes; this wavenumber is about $0.7\, k_0$, where k_0 is the position of the main peak in the static structure factor $S_{NN}(k)$ (cf figure 2), a situation very similar to experimental results for liquid Rb [14]. The reduced sound velocity determined from the initial slope, $c^* = \omega^*/k^*$ (where $\omega^* = \omega a/v_0$) turns out to be 5.0, slightly above the isothermal value $c_T^* = 4.2$. For $x = 0.8$, the sound peak persists up to $k_m^* \simeq 2.3$ and for $x = 0.6$ only up to $k_m^* \simeq 0.3$, while for lower metal concentrations, the sound mode is always overdamped, since it fails to yield a peak in $S_{NN}(k, \omega)$, as already observed in MD simulations of pure salts [15].

Turning to the optic mode, which is signalled by a peak in $S_{ZZ}(k, \omega)$, it is seen to persist in the pure salt up to $k_m^* \simeq 2.4$, where $\omega^*(k = 0) \simeq 18.8 \simeq 1.25\omega_p^*$. The effect of electron screening on the optic mode is seen to be dramatic at $x = 0.2$. The screening of the Coulomb interaction between ions leads to overdamping of the optic mode at small k; the peak in $S_{ZZ}(k, \omega)$ only appears in a narrow wavenumber range around $k^* \simeq 2$, which is of the order of the inverse electron screening length a/λ. For $x = 0.4$ and 0.6 a peak is seen in $S_{ZZ}(k, \omega)$, which may be associated with a coupling between optic and acoustic modes in the region of overlap of their dispersion curves.

This subtle interplay between acoustic and optic branches of the longitudinal excitation spectrum for wavenumbers $k \simeq k_0/2$, deserves further theoretical and experimental investigations.

The authors are indebted to Jean-Louis Barrat for his assistance during the early stages of this work. Parts of this work were carried out while FY was a visiting professor (the Louis Néel chair) at Ecole Normale Supérieure de Lyon, with the support of the Société Lyonnaise de Banque.

References

[1] Edwards P P and Rao C N 1985 *The Metallic and Nonmetallic States of Matter* (London: Taylor and Francis)
[2] Jal J F 1981 1981 *PhD Thesis* Université Claude Bernard, Lyon
Jal J F, Mathieu C, Chieux P and Dupuy J 1990 *Phil. Mag.* at press
[3] Garbade K and Freyland W 1988 *Z. Phys. Chem.* **169**
[4] Fois E, Selloni A and Parrinello M 1989 *Phys. Rev.* B **39** 4812
[5] Hansen J-P and McDonald I R 1986 *Theory of Simple Liquids* 2nd edn (London: Academic)
[6] Chabrier G and Hansen J-P 1983 *Mol. Phys.* **50** 901; 1986 *Mol. Phys.* **59** 1345
[7] Chabrier G, Hansen J-P and Joanny J F 1986 *J. Phys. C: Solid State Phys.* **19** 4443
Chabrier G and Joanny J F 1987 *J. Phys. C: Solid State Phys.* **20** 3787
[8] Parrinello M and Tosi M P 1979 *Riv. Nuovo Cimento* **2** 1
[9] Zerah G and Hansen J-P 1986 *J. Chem. Phys.* **84** 2336
[10] Dixon M and Gillan M J 1981 *Phil. Mag.* B **43** 1099
[11] Jal J F 1991 unpublished
[12] Mathieu C, Jal J F, Dupuy J, Suck J B and Chieux P 1990 *Nuovo Cimento* D **12** 673
[13] De Raedt B and De Raedt H 1978 *Phys. Rev.* B **17** 4344
[14] Copley J R D and Lovesey S W 1975 *Rep. Prog. Phys.* **38** 461
[15] Hansen J-P and McDonald I R 1975 *Phys. Rev.* A **11** 2111